NASA/TP-20240015511

Boron Nitride Nanocomposites for Thermal Management of Aircraft Propulsion System

Marisabel Kelly, Lina Ibrahim, and Diana Santiago
Glenn Research Center, Cleveland, Ohio

Linda S. Mccorkle and Daniel A. Scheiman
University of Toledo, Toledo, Ohio

April 2025

NASA STI Program Report Series

Since its founding, NASA has been dedicated to the advancement of aeronautics and space science. The NASA scientific and technical information (STI) program plays a key part in helping NASA maintain this important role.

The NASA STI program operates under the auspices of the Agency Chief Information Officer. It collects, organizes, provides for archiving, and disseminates NASA's STI. The NASA STI program provides access to the NTRS Registered and its public interface, the NASA Technical Reports Server, thus providing one of the largest collections of aeronautical and space science STI in the world. Results are published in both non-NASA channels and by NASA in the NASA STI Report Series, which includes the following report types:

- TECHNICAL PUBLICATION.
  Reports of completed research or a major significant phase of research that present the results of NASA programs and include extensive data or theoretical analysis. Includes compilations of significant scientific and technical data and information deemed to be of continuing reference value. NASA counterpart of peer-reviewed formal professional papers but has less stringent limitations on manuscript length and extent of graphic presentations.

- TECHNICAL MEMORANDUM.
  Scientific and technical findings that are preliminary or of specialized interest, e.g., quick release reports, working papers, and bibliographies that contain minimal annotation. Does not contain extensive analysis.

- CONTRACTOR REPORT.
  Scientific and technical findings by NASA-sponsored contractors and grantees.

- CONFERENCE PUBLICATION.
  Collected papers from scientific and technical conferences, symposia, seminars, or other meetings sponsored or cosponsored by NASA.

- SPECIAL PUBLICATION.
  Scientific, technical, or historical information from NASA programs, projects, and missions, often concerned with subjects having substantial public interest.

- TECHNICAL TRANSLATION.
  English-language translations of foreign scientific and technical material pertinent to NASA's mission.

Specialized services also include organizing and publishing research results, distributing specialized research announcements and feeds, providing information desk and personal search support, and enabling data exchange services.

For more information about the NASA STI program, see the following:

- Access the NASA STI program home page at http://www.sti.nasa.gov

NASA/TP-20240015511

Boron Nitride Nanocomposites for Thermal Management of Aircraft Propulsion System

Marisabel Kelly, Lina Ibrahim, and Diana Santiago
Glenn Research Center, Cleveland, Ohio

Linda S. Mccorkle and Daniel A. Scheiman
University of Toledo, Toledo, Ohio

National Aeronautics and
Space Administration

Glenn Research Center
Cleveland, Ohio 44135

April 2025

Acknowledgments

The authors gratefully acknowledge the funding support received from the Advanced Air Transportation Technology (AATT) and the assistance provided through the NASA internship program.

This work was sponsored by the Advanced Air Vehicles Program at the NASA Glenn Research Center.

Level of Review: This material has been technically reviewed by expert reviewer(s).

This report is available in electronic form at https://www.sti.nasa.gov/ and https://ntrs.nasa.gov/

NASA STI Program/Mail Stop 050
NASA Langley Research Center
Hampton, VA 23681-2199

Contents

Boron Nitride Nanocomposites for Thermal Management of Aircraft Propulsion System

Marisabel Kelly, Lina Ibrahim,* and Diana Santiago
National Aeronautics and Space Administration
Glenn Research Center
Cleveland, Ohio 44135

Linda S. Mccorkle and Daniel A. Scheiman
University of Toledo
Toledo, Ohio 43606

Summary

Electric aircraft propulsion, utilizing either turbine engines or energy storage systems, is a rapidly advancing aviation technology showing great promise. NASA's Next Generation Air Transportation System (NextGen) initiative is working toward creating a safer, more reliable, and efficient aviation system while minimizing its environmental impact. Thermal management plays a critical role in the design of aircraft propulsion systems. This study examines the effects of varying the form, size, concentration, and processing of boron nitride (BN) fillers on the thermal conductivity (TC) and dielectric strength (DS) of polyimide (PI) films. Multiple forms of BN were investigated to improve the properties of electric cable insulation materials, including hexagonal BN (h-BN), BN nanotubes (BNNT), and BN nanosheets (BNNS). Findings indicate that BNNS produced by the compressible flow exfoliation (CFE) method not only significantly improved the TC of the baseline material (>2×) with an acceptable dielectric breakdown strength (>150 kV/mm) compared with the neat PI, but they also produced a flexible nanocomposite film. This report presents results and discusses the effect of the BN material forms on the TC and DS parameters of BN/PI nanocomposites.

1.0 Introduction

Electrically insulating materials with high thermal conductivity (TC) and dielectric breakdown (DB) voltage are crucial for high-power-density electrical components. The current research addresses a significant practical issue in the power density of electric motors: the poor heat dissipation through the insulation materials in the stator coils. A two-dimensional (2D) convection model was applied to the stator outer surface coils, and the insulation was modeled as a solid material with the conductivity of insulation to understand the effects of the TC of the insulation (i.e., potting material and wire insulation) on the temperature rise in the motor windings (Ref. 1). Figure 1 demonstrates the impact of insulation TC on coil temperature, showing a motor running at a constant current with different slot liner TCs. Increasing the TC of the insulation to greater than 1 W/m·K significantly reduces the operating temperature of the motor, thereby increasing the insulation's life. This also implies that more current could be passed through the identical winding coils without exceeding the temperature rating of the insulation, thereby increasing the motor's output power. These practical implications underscore the importance of this research in aviation technology and materials science, providing valuable insights for engineers and scientists.

NASA has created an extensive portfolio of high-temperature polyimide (PI) materials by developing and using PIs for aerospace and aeronautics applications (Ref. 2). PIs have delivered outstanding performance from aerospace engines to power electronics because of their high-temperature tolerance, flexibility, and chemical and mechanical resistance. High-temperature PIs have been influential in developing novel materials such as multifunctional composites, foams, and aerogels (Refs. 3 to 5). PIs are also used in many electrical devices, from tiny capacitors to giant generators. The state-of-the-art polymeric insulation materials for low-voltage (50 to 1,000 Vac) motors and generators include modified polyurethane (thermoplastic) bond coat, modified polyurethane, and modified polyester imide; for high-voltage components (>1,000 Vac), these include poly-ethylene terephthalate (PET)/mica and PI film, commonly used for traction and high-temperature motors (Ref. 6). PI remains

*NASA Office of STEM Engagement Summer 2024 Intern, Stanford University undergraduate.

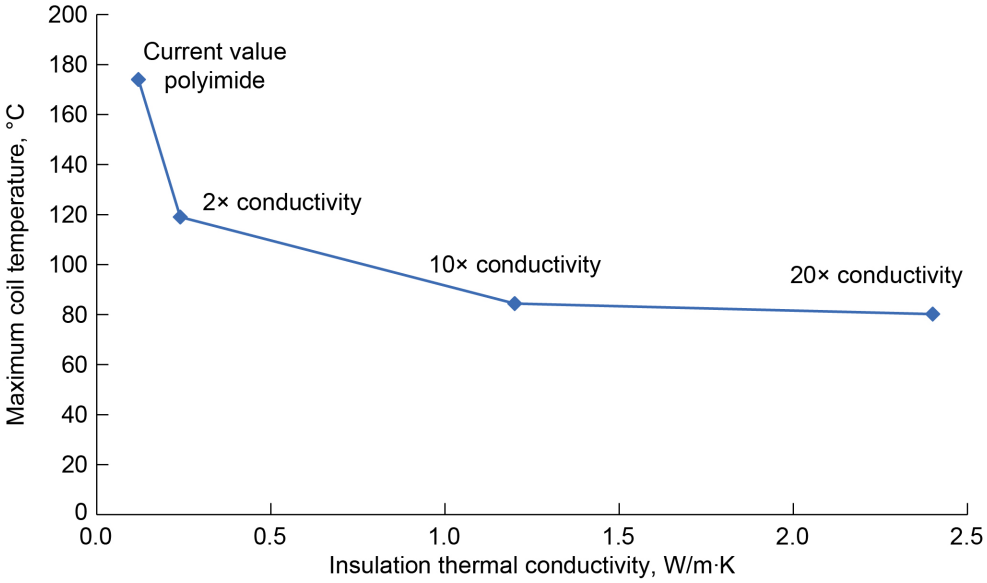

Figure 1.—Effect of insulation TC on motor stator coil temperature; power loss (I^2R) = 1.8 kW and heat transfer coefficient (h_{cool}) = 5,000 W/m^2·K.

stable across various temperatures, from –269 to 400 °C (~4 to 673 K), but it possesses relatively low TC (i.e., 0.2 to 0.5 W/m·K) (Ref. 7).

Research has been directed toward improving the TC in electrical insulation materials currently used on electric machines (i.e., epoxy, thermoplastic, and thermoset polymers) by adding inorganic fillers with high TC properties to address the heat dissipation challenge. BN is a unique material with high TC that is still electrically insulating. The 2D hexagonal BN (h-BN) and its derivative forms (e.g., BN nanotubes (BNNT) and nanosheets (BNNS)) are excellent candidates for inorganic fillers because of their high TC, excellent electric insulation capabilities, and low dielectric constant. For example, the reported in-plane TC of h-BN is higher than 200 W/m·K, and its through-plane TC is about two orders of magnitude lower (Ref. 8). The measured TC for BNNT is ~350 W/m·K (Ref. 9). In addition, BNNT are one of the best dielectric materials available, with a band gap of ~5 eV (Ref. 10). Exfoliation of h-BN produces BNNS (here, "nano" refers to the thickness of the sheet rather than its lateral size). Studies have indicated that BNNS have an in-plane TC with calculated room-temperature values of more than 600 W/m·K (Ref. 11) and that it is higher than their through-plane TC.

Polymeric nanocomposites made with fillers such as BN, aluminum oxide (Al_2O_3), aluminum nitride (AlN), and silica (SiO_2) have been studied to improve polymer matrix properties. For example, a TC of 32.5 W/m·K has been reported for a BN-filled (225 μm) polybenzoxazine at its maximum filler loading of 78.5 vol% (88 wt%) (Ref. 12). A TC of 19 W/m·K was also found for an epoxy composite containing 27 vol% h-BN and cubic boron nitride (c-BN) with particulate sizes of 0.6 and 0.1 μm, respectively (Ref. 13). However, the DB strength performance was not investigated; in many cases, introducing high filler loadings in a polymer to increase the TC does not lead to satisfactory dielectric properties, primarily due to voids or particle agglomerates that form in the microstructure of the composite and on the surface.

This report presents fundamental investigations on developing PI (with a maximum use temperature of 240 °C) nanocomposites with BN particles to study the effect of filler type, filler loading, and processing on their TCs and DB strengths. The findings are used as a guide to identify promising material formulations for electric-powered aircraft, based on the electric motor types and generator insulation requirements.

2.0 Experimental Procedures

2.1 Materials

The PT110 h-BN powder used had an average particle size of ~45 μm (Ref. 14). BNNT were prepared and purified in house using a modified chemical vapor deposition (CVD) technique developed at the NASA Glenn Research Center (Refs. 15 and 16). Two different exfoliation methods were used to obtain BNNS: in-house chemical exfoliation (CE) and compressible flow exfoliation (CFE). Those from the latter technique were purchased directly from an outside lab (Refs. 17 and 18). The following reagents and solvents were purchased commercially

and used without further purification: pyromellitic dianhydride (PMDA), oxydianiline (ODA), anhydrous nitrogen, N-dimethylacetamide (DMAc), ethanol (EtOH), 3-aminopropyl-triethoxysilane (APTES, 50 percent in EtOH), nitric acid (65 wt% solution HNO_3), and Defloc Z3 dispersing agent (DA).

2.2 Equipment and Characterization

Polyamic acid (PAA, a PI precursor) films were obtained by casting onto an uncoated Mylar® (DuPont Teijin Films U.S.) film and setting the film thickness with an adjustable doctor blade. Prior to film casting, sample solutions (e.g., PAA on DMAc with BN particles) were mixed using one or a combination of the following mixing techniques: ultrasonication, an ultrasonic water bath, and a centrifugal mixer. All thicknesses of the processed films were measured using a digital caliper. Specific heat and thermal diffusivity were measured at 25 °C. The test method followed to obtain TC was ASTM E1461–13, the Standard Test Method for Thermal Diffusivity by the Flash Method (Ref. 19). Samples of the PI composite films (dimensions 10- by 10-mm squares with an average thickness of 0.1 mm) were coated with a thin film of gold and a second coating of graphite and then tested. DB voltages were tested in accordance with ASTM method D149–09, the Standard Test Method for Dielectric Breakdown Voltage and Dielectric Strength of Solid Electrical Insulating Materials at Commercial Power Frequencies (Ref. 20). Round 1-in.-diameter samples were tested individually at a voltage ramp rate of 0.6 kV/s using a 0.25-in.-diameter electrode. Either electrical tape was used or the sample was submerged in oil to prevent air gaps. Up to five 1-in. rounds were tested from each film. Film thicknesses ranged from 0.01 to 0.2 mm. The DB obtained for all films tested was normalized using the average thickness of each sample. Scanning electron micrograph (SEM) images were collected using an operating voltage of about 6 KeV. Raman spectra were collected using a 633-nm laser. Fourier transform infrared (FTIR) spectra were collected using an Agilent Cary 670 spectrometer and Pike Technologies ATR (attenuated total reflection) with a MIRacle™ performance diamond plate. Thermogravimetric analysis (TGA) was performed by ramping samples from room temperature to 900 °C at 10 °C/min in either a nitrogen or air atmosphere. Heat capacities (C_p) were measured using a differential scanning calorimeter (DSC).

2.3 Synthesis and Processing

2.3.1 General Synthesis of PI Precursor, PAA

PAA solution was prepared using a previously published method (Ref. 21). ODA (2.00 g, 10 mmol) and DMAc (25 mL) were added into a 250-mL three-necked round-bottom flask with a magnetic stirrer under nitrogen. After ODA was dissolved entirely, PMDA (2.18 g, 10 mmol) was added and stirred overnight (12 to 18 h). An amber, viscous PAA solution was obtained.

2.3.2 Functionalization of In-House-Prepared BNNT and CE BNNS

A previously published method was used to functionalize inhouse-prepared BNNT and CE BNNS (Ref. 22). The BN particles were dispersed in an HNO_3 solution (65 wt%), achieving a final concentration of 1 mg/mL, and then sonicated (water bath sonicator) for 6 h. This preliminary step was taken to introduce OH functional groups on the surface of BNNT (F-BNNT) or CE BNNS (CE F-BNNS). After three washing steps by ultracentrifugation in absolute ethanol, the samples were sonicated for 12 h in APTES. Next, they were rinsed with deionized water and dried overnight in the oven at 110 °C.

2.3.3 Preparation of PI Nanocomposite Films With h-BN, F-BNNT, CE F-BNNS, or a Combination Thereof

Nanocomposite films of PI and BN fillers (i.e., h-BN, F-BNNT, and CE F-BNNS) were prepared by mixing the PI-precursor PAA solution with BN fillers at the respective weight ratio per sample specification. The heterogeneous solution was dispersed using ultrasonication for 15 to 30 min (5 min on, 10 min off) at an operation frequency of 40 kHz and with an ice bath to stabilize the temperature. Up to three processing cycles may be required for proper dispersion of BN particles when using a large amount of BN fillers (i.e., 10 wt% or more). The resulting heterogeneous solution of PAA and BN filler was cast. The film was dried under a fume hood (25 °C) for 12 to 24 h to allow the solvent to evaporate. The resulting nanocomposite film was transferred to a programmable oven for thermal imidization (curing process) at 100, 200, and 350 °C, each for 1 h with a ramp time of 30 min. This process converted the PAA-BN to the cured PI/BN nanocomposite film.

2.3.4 Preparation of Nanocomposite Films With h-BN, F-BNNT, CE F-BNNS, or a Combination Thereof, Using Defloc Z3

DMAc (32.68 mL, 30.73 g) and the Defloc Z3 DA (0.5 or 5 wt%, per sample specification) were placed into a 120-mL glass beaker with a magnetic stirrer and stirred for a couple of minutes. BN fillers (i.e., h-BN, F-BNNT, and CE F-BNNS, wt% based on PAA solution, per sample specification) were added to a beaker in an ice bath (to control temperature generated from the process) and dispersed using ultrasonication for 15 to 30 min (5 min on, 10 min off) at an operation frequency of 40 kHz. ODA (4.00 g, 20 mmol) was added, and the solution was stirred magnetically at ambient temperature (25 °C) under nitrogen until the ODA was fully dissolved. PMDA (4.36 g, 20 mmol) was added slowly while stirring. The solution was stirred until no particles were visible (12 to 18 h), and a viscous PAA-BN heterogenous solution was obtained. Before casting, the PAA-BN solution was mixed again for 5 to 15 min. A film was cast onto an uncoated Mylar® film, and the thickness was controlled by using an adjustable doctor blade. The film was placed under the hood for 12 to 24 h to allow the solvent to evaporate. The dried BN/PAA nanocomposite film was placed in a programmable oven, as previously described in Section 2.3.3, to obtain the BN/PI nanocomposite film.

2.3.5 Preparation of Nanocomposite Film of PI With CFE BNNS

The (CFE BNNS)/PI nanocomposite film was prepared by mixing the PI-precursor PAA solution with CFE BNNS at the respective weight ratio, per sample specification. The heterogeneous solution was added to a beaker in an ice bath and placed in an ultrasonicator for 15 to 30 min of total process time (e.g., 5 min on with 10 min off) at an operation frequency of 40 kHz. The resulting heterogeneous solution of PAA and CFE BNNS was cast onto an uncoated Mylar® film using an adjustable doctor blade. The (CFE BNNS)/PAA nanocomposite film was dried under a fume hood (25 °C) for 12 to 24 h to allow the solvent to evaporate. The resulting nanocomposite film was transferred to a programmable oven for thermal imidization, as described in Section 2.3.3, to obtain (CFE BNNS)/PI nanocomposite film.

3.0 Results and Discussion

The TC and DB of the resulting PI nanocomposites using BN fillers such as h-BN, BNNT, and BNNS at various weight percentages (wt%) are presented and discussed here. Table I summarizes the types of BN fillers, their respective synthesis processes, and the loading levels used. Figure 2 displays SEM images of the BN types. Commercially available h-BN (Figure 2(a)) was acquired with a particle size of ~45 μm and layer thickness ranging from 2 to 5 μm. The CVD BNNT synthesized in house had diameters ranging from 20 to 50 nm and lengths in the micron range (Figure 2(b)). Layer thickness for in-house CE BNNS produced was approximately 20 to 50 nm (Figure 2(c)). For CFE BNNS (Figure 2(d)), the layer thickness ranged from 2 to 10 nm.

BNNS prepared by CE (Figure 2(c)) show vertical stacking of nanosheets promoted by weak intermolecular forces, including van der Waals forces and instantaneous dipole-induced dipole forces, characteristics of 2D honeycomb lattices of firmly bound boron and nitrogen atoms (Ref. 23). In the case of CFE-prepared BNNS, a higher surface area was achieved because of smaller BN particle sizes, reducing the number of layers.

BN fillers were added directly to the PAA solution and dispersed using ultrasonication. PAA is typically compatible with dipolar aprotic solvents, which makes it convenient to integrate BN fillers before thermal imidization. However, a stable dispersion within an inorganic filler and polymeric matrix solution is still challenging to achieve (Ref. 23). Initially, some precipitation was observed at the bottom of the flask after a couple of minutes with the addition of either h-BN or CE BNNS. Acceptable dispersion was achieved with samples of BNNT; however, the viscosity rapidly increased, posing challenges for dispersion at higher loading levels. Additionally, after casting, particulate agglomeration was observed.

TABLE I.—SUMMARY OF PI-NANOCOMPOSITE AND PI-COMPOSITE SYSTEMS INVESTIGATED

Polymeric matrix	BN filler type	Synthesis process	Loading, wt%
PI	BNNT	CVD	10, 12, 17, 20
	F-BNNS[a]	CE	10
	F-BNNT and F-BNNS	CVD, CE	10/10
	h-BN	CA	20, 60
	h-BN and F-BNNT	CA, CVD	10/2
	h-BN and F-BNNT	CA, CVD	10/10
	BNNS	CFE	7, 14, 24, 34

[a]Functionalized with APTES.

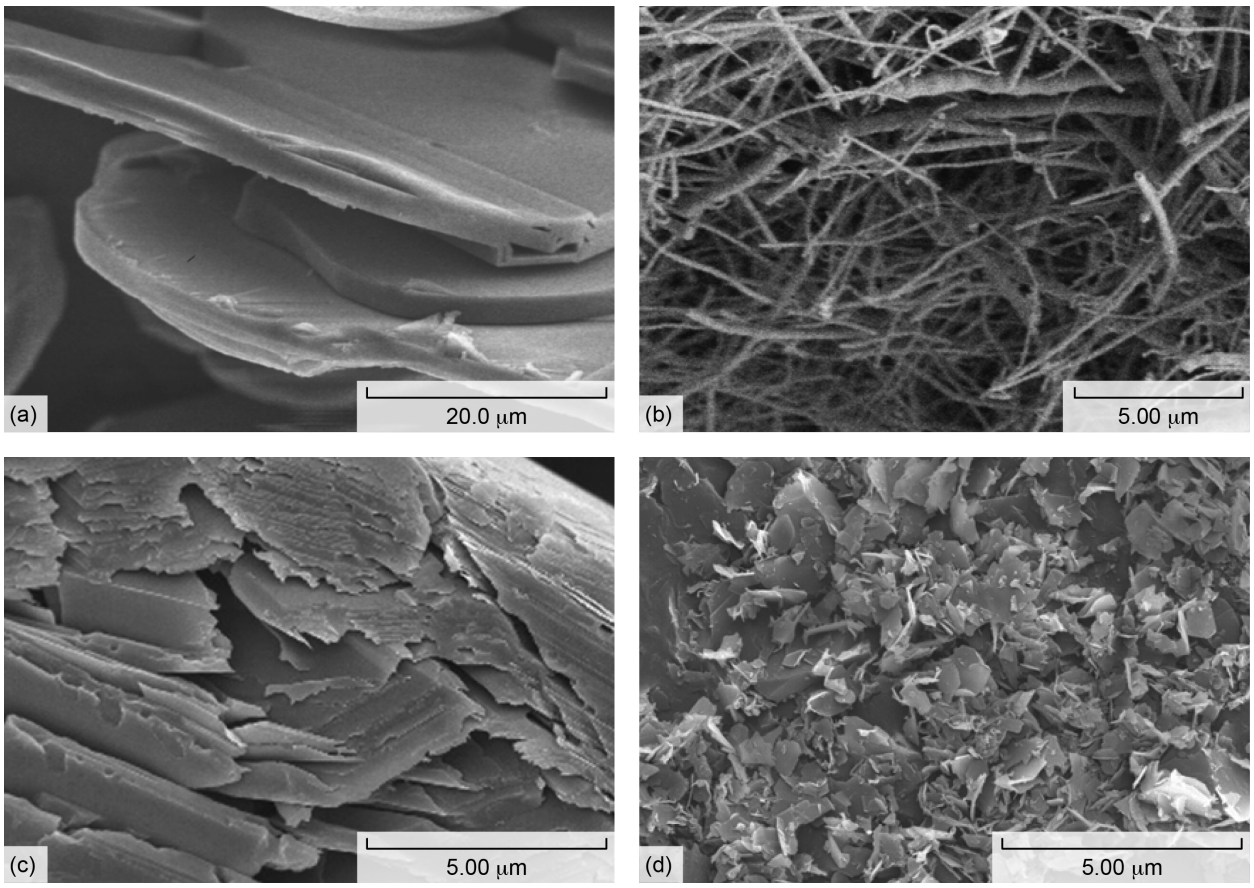

Figure 2.—SEM images of BN forms. (a) h-BN. (b) BNNT. (c) CE BNNS. (d) CFE BNNS.

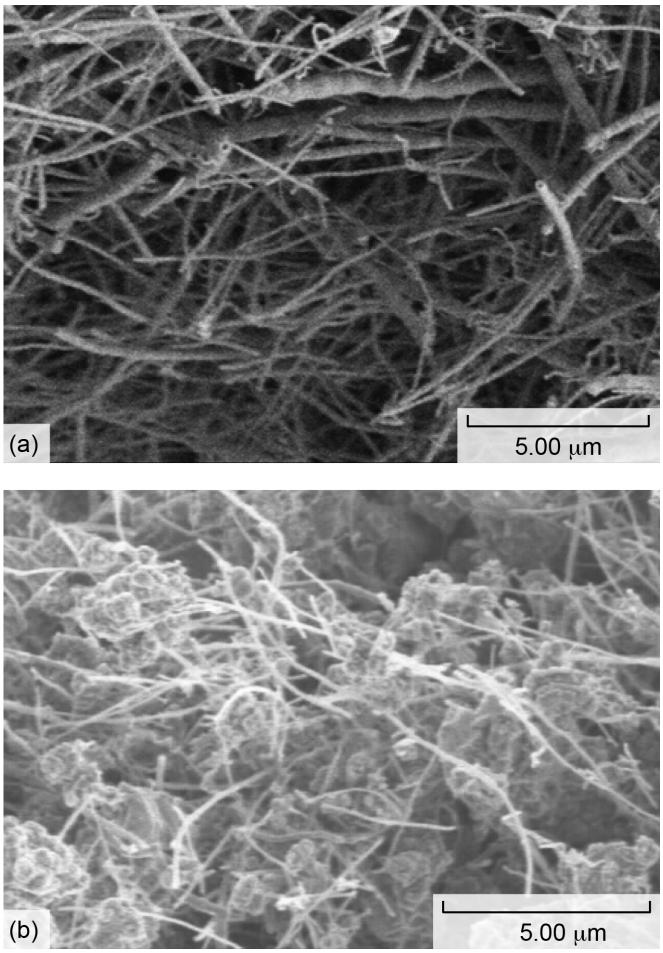

Figure 3.—SEM images of BNNT filler. (a) As prepared. (b) Functionalized with APTES (F-BNNT).

Surfaces of the BNNT and CE BNNS were functionalized using APTES following the reported method described in Section 2.3.2 to enhance dispersion in the PAA solution. Functionalization reduces particle agglomeration and minimizes Van der Waals forces for better dispersion. Both functionalized materials were extensively characterized by infrared. Figure 3 shows SEM images of before (Figure 3(a)) and after (Figure 3(b)) functionalization.

Table II summarizes the composite films with different weight percentages and their respective TCs. The data show the most significant increases in TC occurred when functionalized nanoparticles were used. Adding 12 wt% h-BN did not improve TC of the neat PI (no fillers). One contributing factor to this result is the insufficient particle-to-particle contact to improve phonon transport and thus increase TC. As previously reported in the literature, the filler's properties cannot adequately transfer to the polymer matrix if these interactions are ineffective

TABLE II.—EFFECT OF BN FILLER TYPE AND CONCENTRATION ON TC OF PI NANOCOMPOSITE FILMS

Filler	Concentration, wt%	TC, W/m·K
No filler	0	0.12±0.01
h-BN	12	0.11±0.01
F-BNNS[a]	10	0.30±0.02
F-BNNT and F-BNNS[a,b]	10/10	0.29±0.02
F-BNNT[b]	10	0.79±0.04
F-BNNT[b]	12	0.91±0.03
F-BNNT[b]	17	0.93±0.05
F-BNNT[b]	20	1.59±0.08

[a]Prepared in house by CE followed by functionalization.
[b]Prepared in-house using modified CVD method followed by functionalization.

or absent (Ref. 24). Another critical factor is processing. The nanocomposite should, ideally, have no microscopic voids or very minimal voids. The appearance of microscopic voids depend on several factors, including how the nanocomposite is processed (i.e., mixing, casting, hot pressing, curing, etc.), concentration, size, shape of fillers, particle agglomerates, and interfacial mismatch (Ref. 25). In this case, the presence of voids or large interfaces leads to more air gaps and thus more phonon scattering, which ultimately suppressed thermal conduction.

TC increases were observed using either F-BNNS or a combination of F-BNNT and F-BNNS (each 10 wt%). For these nanocomposite films, an improvement of more than 2× was obtained. The SEM images revealed that functionalized BNNT were well distributed throughout the sample (Figure 4). However, BNNS were only partially well distributed: areas with BNNS were found to restack due to Van der Waals forces and instantaneous dipole-induced dipole interactions (Figure 4(a)), despite functionalization allowing for microscopic voids.

Significant improvement in TC was achieved using F-BNNT at 10, 12, 17, and 20 wt%. Figure 5 displays the TC plot as a function of F-BNNT weight percent. F-BNNT/PI at 10 wt% content achieved a TC improvement of >6×. By increasing F-BNNT content to 12 and 17 wt%, the TC improvement was >7× compared to the neat PI.

SEM images were obtained for the 12-wt% F-BNNT/PI nanocomposite film (Figure 6). The sample surface (Figure 6(a)) and the cut cross section (Figure 6(b)) show uniformly distributed F-BNNT. Obtaining an actual fracture surface was impossible because the thin film was very tough and would not produce a clean fracture.

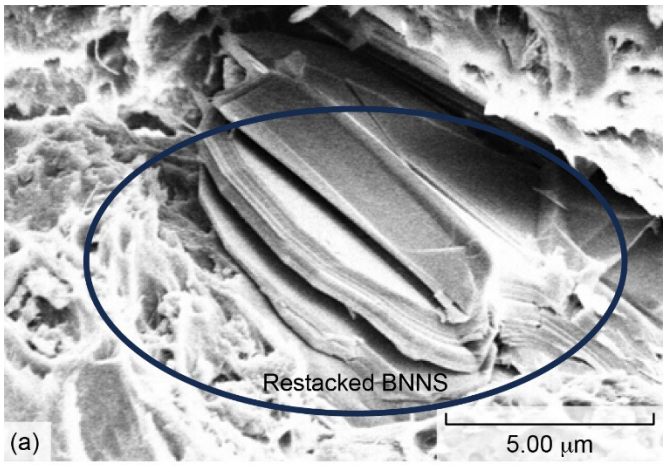

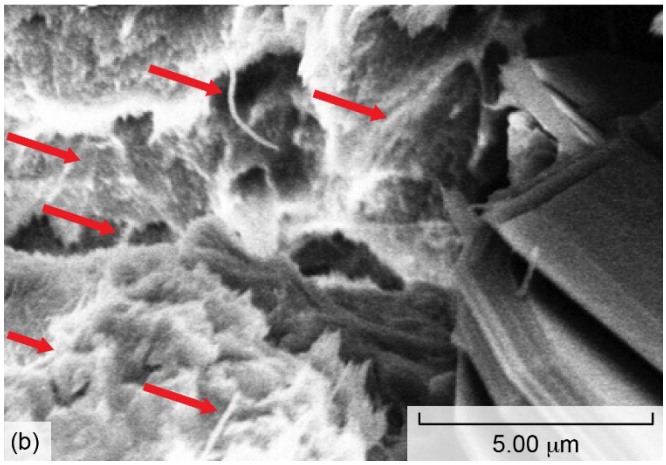

Figure 4.—SEM images of F-BNNT(10 wt%)/F-BNNS (10 wt%)/PI nanocomposite film. (a) Restacked nanosheets. (b) Higher magnification image. Arrows show F-BNNT in polymer matrix.

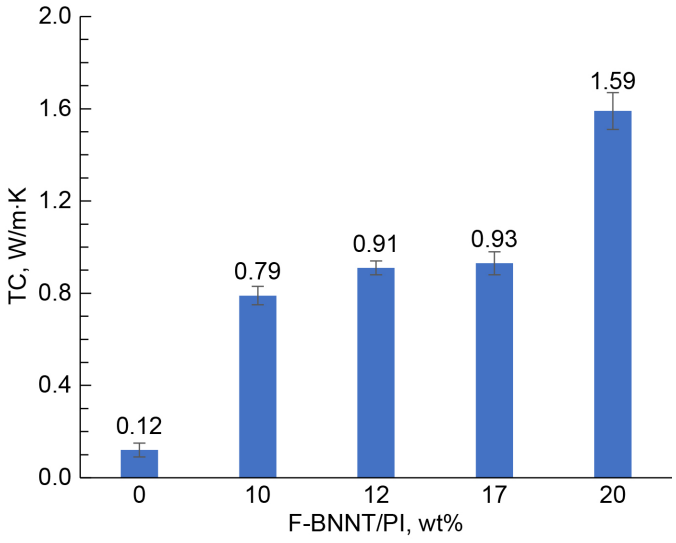

Figure 5.—Thermal conductivity of F-BNNT/PI as function of F-BNNT weight percent.

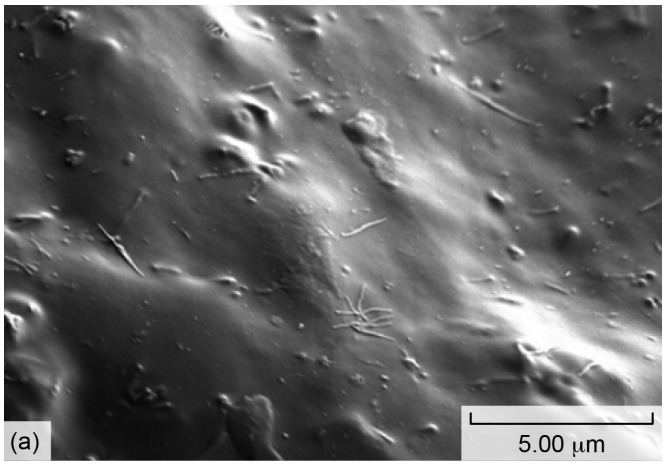

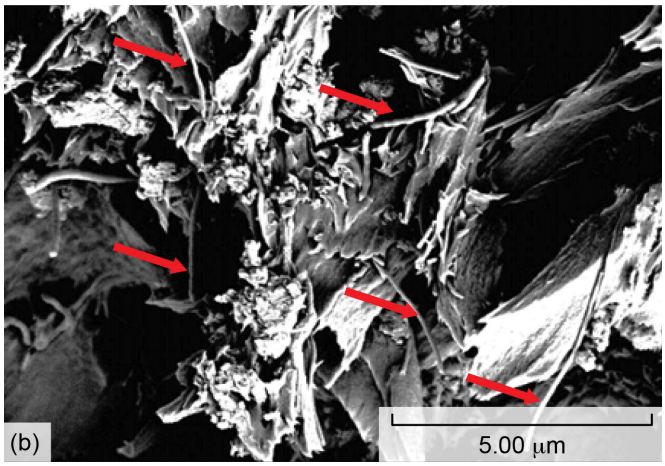

Figure 6.—SEM images of F-BNNT/PI nanocomposite at 12 wt% F-BNNT. (a) Surface view. (b) Cross-sectional view. Arrows identify F-BNNT.

The highest TC of 1.59 W/m·K was obtained for 20 wt% PI/F-BNNT, which is equivalent to a 13-fold improvement. However, these films were observed to become less flexible.

The next approach used exfoliated BNNS produced by the CFE method. The CFE method efficiently produces high-quality 2D BNNS at high throughput. X-ray diffraction (XRD) and Raman spectroscopy were used to characterize the baseline properties of the CFE BNNS; very low variation in the batch-to-batch consistency was found for the BNNS produced by this method.

(CFE BNNS)/PI nanocomposite films were prepared at 7, 14, 24, and 34 wt%. The inset in Figure 7 is a digital image of the 24 wt% film, showing its flexibility with no cracks when bent. Figure 7 compares each nanocomposite film's TC. As the CFE BNNS content increases, TC improves compared to the neat PI: adding 14 wt% doubled the TC compared to that of the neat PI, and there is a TC increase of 6× for the 24 wt% nanocomposite. The highest TC was obtained for the 34 wt% (CFE BNNS)/PI nanocomposite of 2.53 W/m·K, representing an increase of 20×.

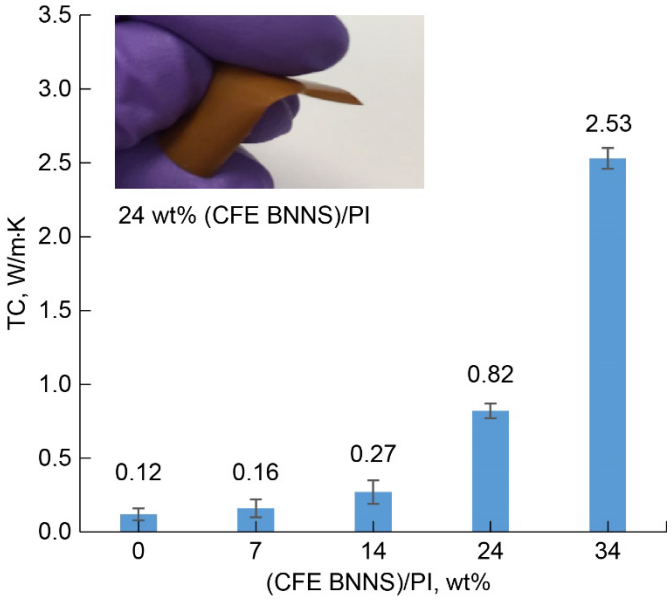

Figure 7.—TC as function of (CFE BNNS)/PI concentration and digital image of 24 wt% nanocomposite film.

Figure 8 shows SEM images for (CFE BNNS)/PI at 24 wt%. Well-distributed CFE BNNS can be observed throughout the film's cross section and surface in Figure 8(a) and Figure 8(b), respectively. The CFE BNNS combined with the PAA solution had better dispersion, resulting in a more consolidated structure with minimal microvoids. The findings remained consistent for the 34 wt% (CFE BNNS)/PI nanocomposite film.

DB occurs when the voltage across an electrically insulating material exceeds a threshold, causing a dramatic drop in electrical resistance and a nearly unrestricted flow of electrical current across the material (in the direction of the electric field). Sample thickness, defects, and imperfections influence the breakdown (Ref. 26).

In this case, Defloc Z3 was used as a DA to improve dispersion and obtain better suspended BN fillers to avoid precipitation and agglomerations during casting. Defloc Z3 is a triglyceride typically used as a deflocculant to help disperse inorganic particles to form a stable solution. The synthesis of the PAA was carried out in situ with BN fillers. Adding DA significantly improved the BN particle suspension, allowing the production of a thin film by casting with no filler precipitation observed.

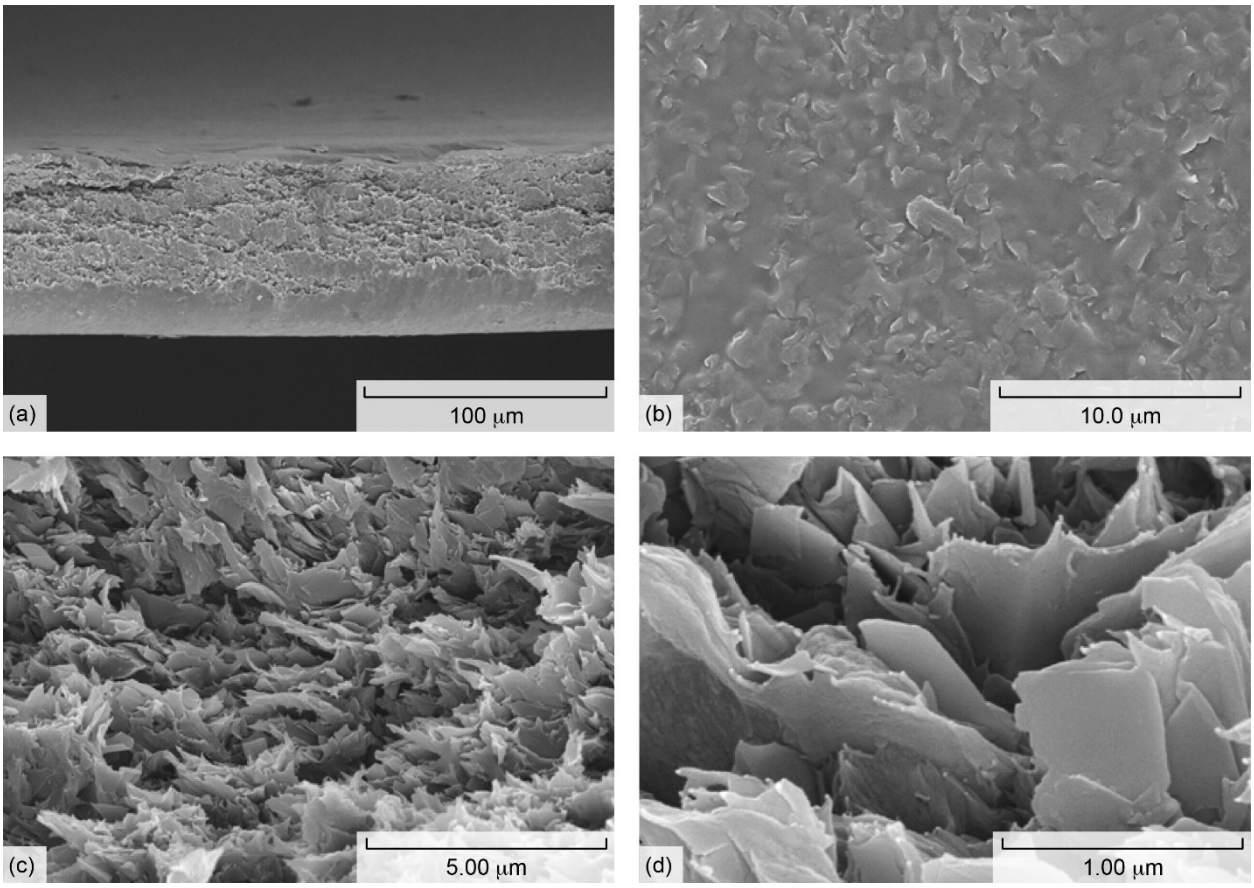

Figure 8.—SEM images of 24 wt% (CFE BNNS)/PI nanocomposite. (a) Cross-sectional view. (b) Surface view. (c) Cross-sectional view at higher magnification. (d) Cross-sectional view at still higher magnification.

TABLE III.—DIELECTRIC STRENGTH OF PI AND BN/PI COMPOSITE FILMS

Film[a]	Film thickness,[b] mm	DA,[c] wt%	DS,[d] kV/mm
PI neat	0.05	0	175±16
	0.11	0	100±3
PI-DA	0.05	0.5	164±20
	0.13	0.5	82±6
DA	0.05	5.0	155±22
	0.10	5.0	83±12
h-BN/(PI-DA), 20 wt%	0.05	0.5	95±27
h-BN/(PI-DA), 20 wt%	0.10	0.5	67±19
h-BN/(PI-DA), 60 wt%	0.14	0.5	42±8
h-BN/(PI-DA), 60 wt%	0.10	5.0	69±7
h-BN(10 wt%)/ F-BNNT(2 wt%)/ (PI-DA)	0.13	5.0	80±3

[a]BN filler content is measured as the weight percentage of the ODA-PMDA mass.
[b]Thickness average.
[c]DA Defloc Z3 content is measured as weight percentage of DMAc solvent mass.
[d]DS is average of five films.

Table III summarizes the DB strength in BN/PI films. Typically, higher dielectric strength (DS) is expected for thin films. In this case, DS for neat PI films of 0.05 and 0.1 mm thicknesses was 175 and 100 kV/mm, respectively (Table III). The effect of varying DA concentrations on DS was also studied for neat PI films. A DS of 164 kV/mm was obtained for a PI film containing 0.5 wt% DA (thickness of 0.05 mm). This represents a 6.5 percent decrease in DS compared to the neat PI of similar thickness. A lower DS, 82 kV/mm, was obtained for PI films with a thickness of 0.1 mm and 0.5 wt% of DA compared to that of the neat PI film at a similar thickness. Based on these results, it is noted that the DA affects the DS of the PI film. The decrease in DS for samples containing the DA could be attributed to the bonds in the DA becoming more polarized in the electric field; as these polar bonds become more strained in the electric field, the polarization of the composite increases, leading to faster DB.

Figure 9 compares the DS and the weight percentage of BN fillers for film thicknesses of 0.05 and 0.1 mm. Most PI films with various BN fillers and DA concentrations have lower DS than PI-DA. For 20 wt% h-BN/(PI-DA) (0.5 wt%), a 95 kV/mm DS was obtained, representing a 53 percent decrease in DS compared to that of the PI-DA with a thickness of 0.05 mm.

It was observed that in the case of films at 0.1 mm thickness, increasing the DA content from 0.5 to 5 wt% increased the DS from 42 to 69 kV/mm for films containing h-BN at 60 wt%. The best results were achieved with the composite film h-BN (10 wt%)/F-BNNT (2 wt%)/(PI-DA): only a 4 percent decrease in DS was observed compared to that of the PI-DA (5 wt%). Also, adding 2 percent of just F-BNNT improves the DS and helps to overcome the decrease in DS generally observed with the increase of DA in PI-DA samples.

SEM images of PI films were obtained to evaluate the h-BN/PI surface and cross section. Figure 10 shows SEM images corresponding to a PI-DA (0.5 wt%) film (Figure 10(a)), a PI-DA (0.5 wt%) film containing 60 wt% h-BN (Figure 10(b)), and the cut cross section of the sample shown in Figure 10(b) (Figure 10(c)). The SEM image of PI-DA (0.5 wt%) in Figure 10(a) appears smoother than the PI sample containing h-BN in Figure 5(b), revealing surface imperfections in the latter. Moreover, a close look at the cross section reveals voids. Lower breakdown voltage of the composites can be attributed to the sample surface imperfections and voids.

In contrast, a good dispersion and stable suspension were obtained for CFE BNNS when mixed with PAA solution without the need for dispersion agents. The DB strength of the (CFE BNNS)/PI nanocomposite was more consistent, as seen in Figure 11. The decrease in DS for the 24 and 34 wt% (CFE BNNS)/PI nanocomposites (thickness of 0.02 mm) was observed to be 7 and 12 percent, respectively. For the 24 wt% (CFE BNNS)/PI sample, the DS for nanocomposites of 0.05 and 0.07 mm thickness was 138 and 129 kV/mm, respectively. This corresponds to a 24 and 29 percent decrease compared to that of the neat PI.

SEM images of PI films were obtained to evaluate the surface and cross section of 24 wt% (CFE BNNS)/PI. Figure 12 shows SEM images of the surface of neat PI and both the surface and cut cross section views of the 24 wt% (CFE BNNS)/PI nanocomposite sample. A more uniform surface (Figure 12(b)) and well-distributed CFE BNNS (Figure 12(c)) can be observed throughout the film's surface and cross section, resulting in a more consolidated structure with minimal microvoids. This allows the properties of the BNNS to be transferred more efficiently through the polymeric matrix without the need for chemical functionalization or a DA.

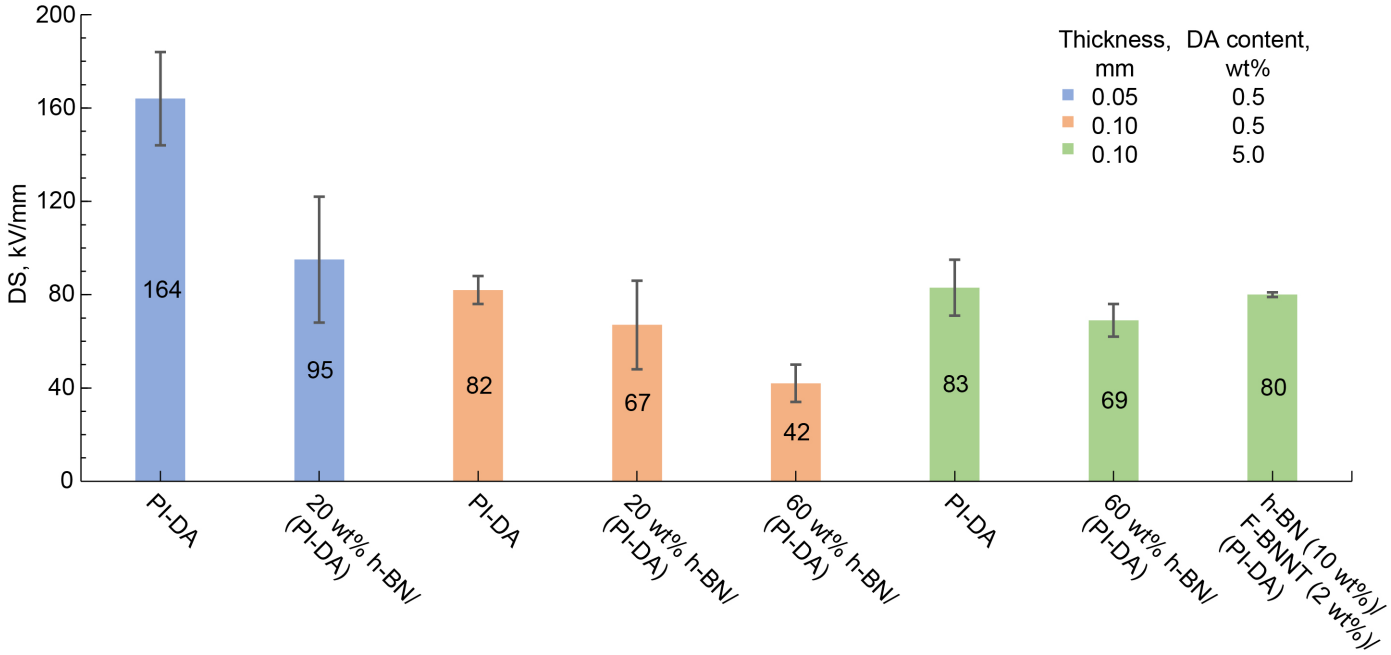

Figure 9.—Variation of DS with weight percent of BN fillers for PI-DA composite films of varying DA content and thickness.

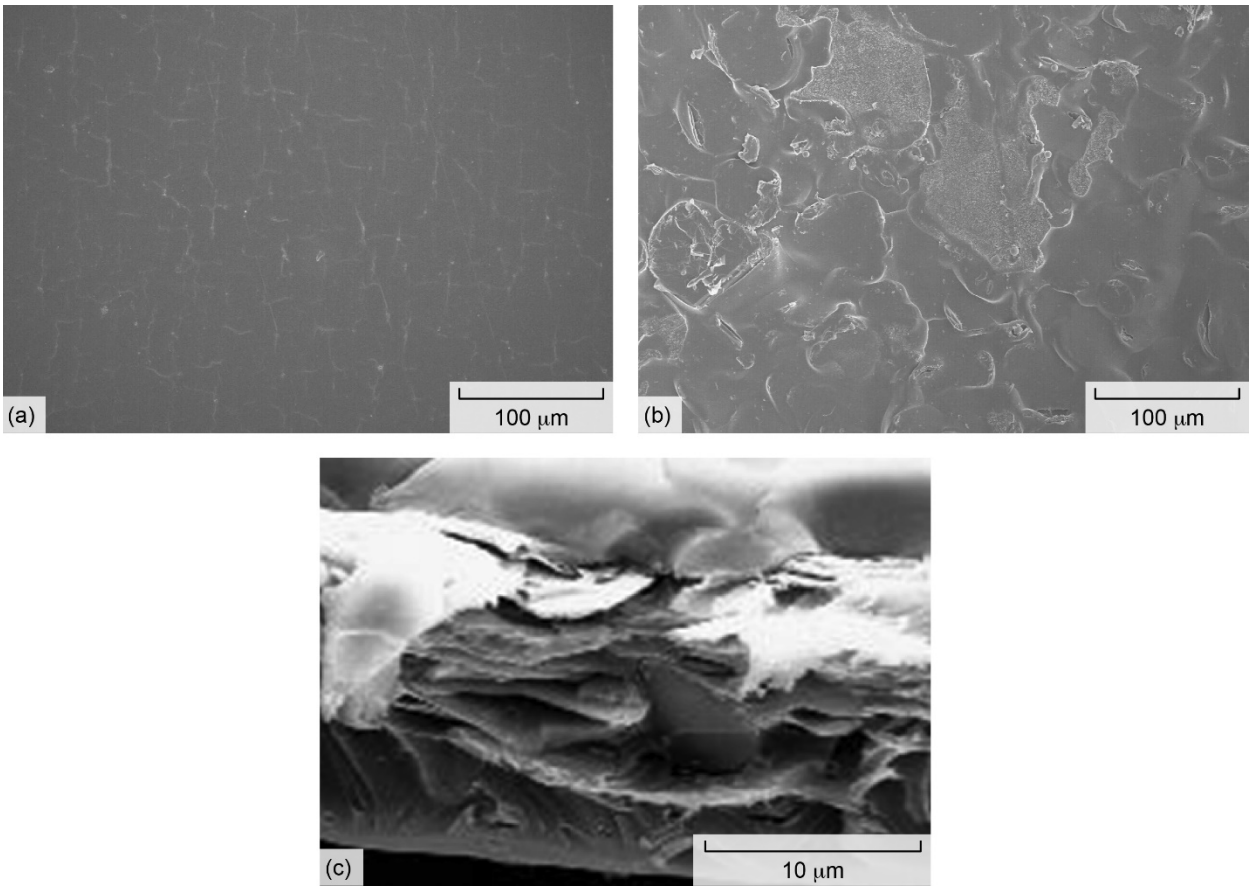

Figure 10.—SEM images of PI-DA films. (a) Surface view of PI-DA (0.5 wt%). (b) Surface view of h-BN (60 wt%)/(PI-DA) (0.5 wt%). (c) Cross-sectional view of h-BN (60 wt%)/(PI-DA) (0.5 wt%).

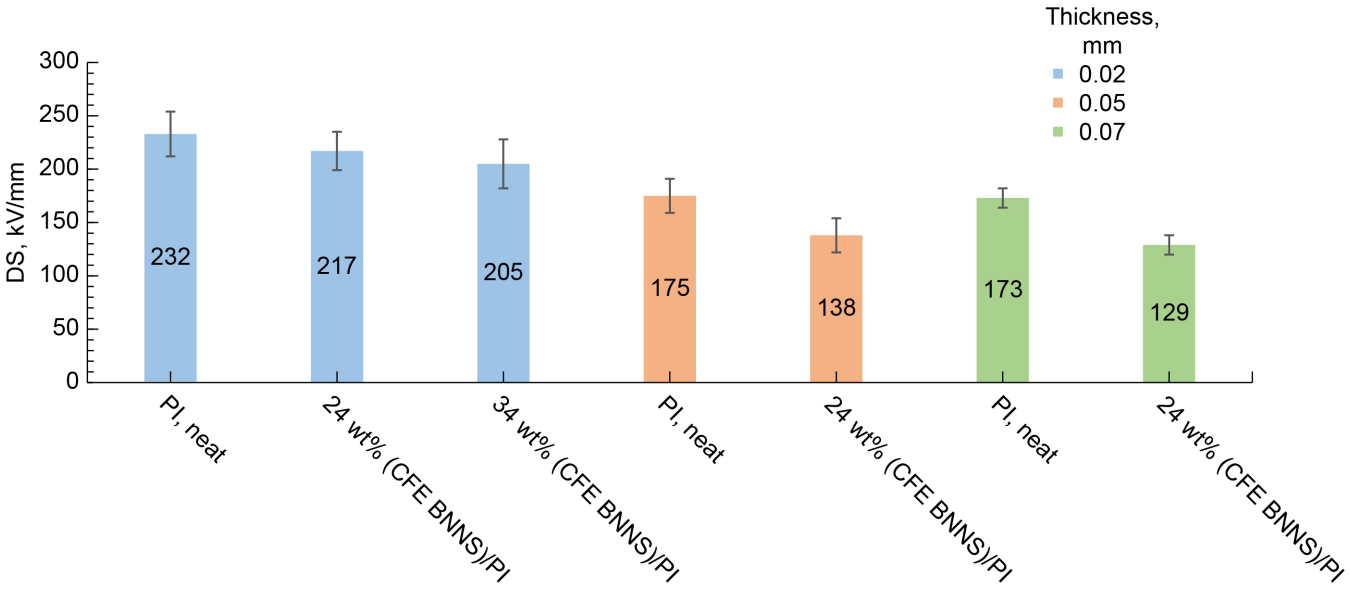

Figure 11.—Effect of filler concentration and thickness on DS of CFE BNNS at film thicknesses of 0.02, 0.05, and 0.07 mm.

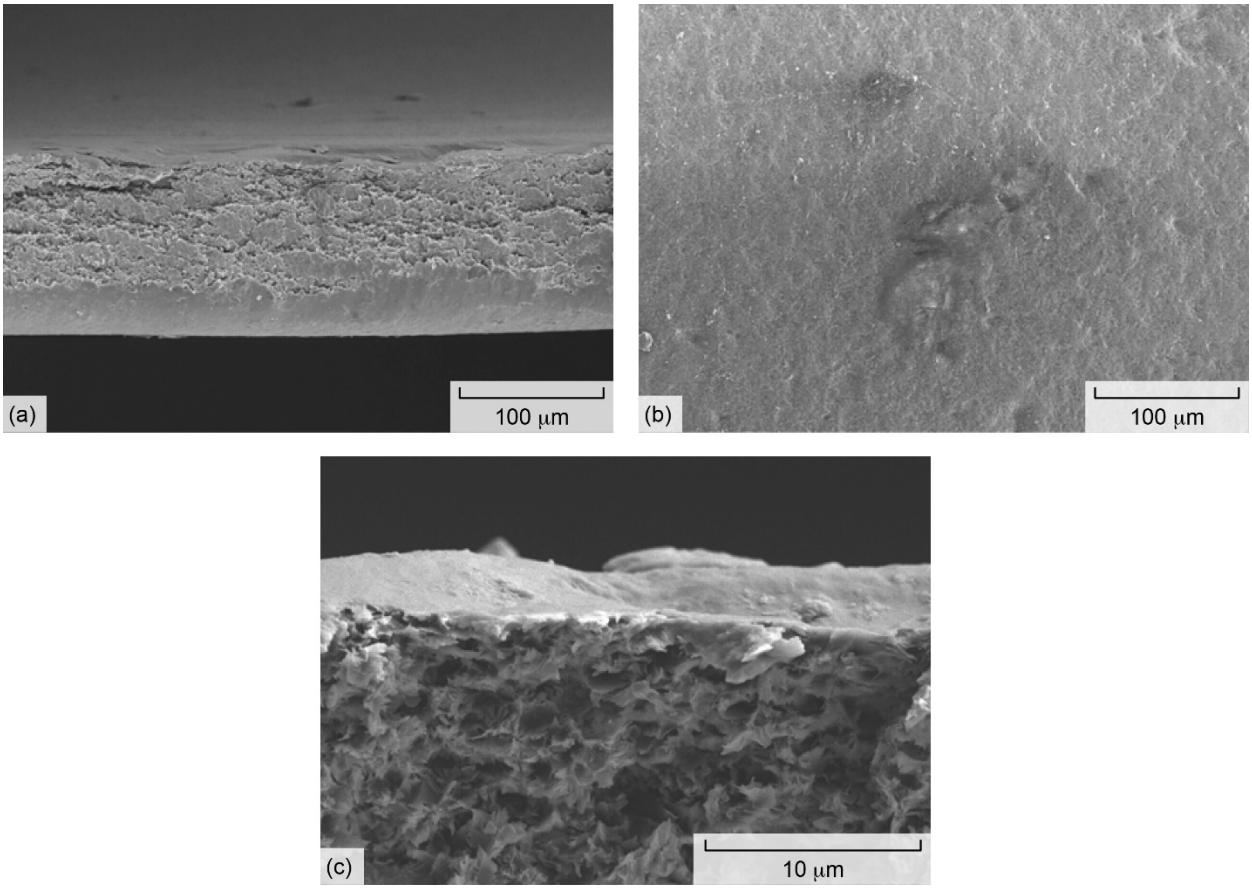

Figure 12.—SEM images of 24 wt% (CFE BNNS)/PI films. (a) Surface view of neat PI. (b) Surface view of 24 wt% (CFE BNNS)/PI. (c) Cross-sectional view of 24 wt% (CFE BNNS)/PI.

4.0 Conclusions

This report discussed the effects of boron nitride (BN) filler type and loading on the thermal conductivity (TC) and dielectric strength (DS) of polyimide (PI) composite films containing either nano- or micrometer-size fillers or a combination of both. In-house-prepared BN nanotubes (BNNT) and BN nanosheets (BNNS) prepared by chemical exfoliation (CE BNNS) needed to be functionalized for better distribution throughout the polymer matrix to improve TC and DS. In general, TC increases with the addition of the inorganic particles if there is sufficient phonon transport. BNNS prepared using the compressible flow exfoliation (CFE) method show better dispersion without chemical functionalization. TC significantly increased when CFE BNNS were added to the PI. However, adding a dispersing agent (DA) and BN fillers for an in situ synthesis of the polyamic acid (PAA) solution did not result in an improvement in the DS properties of the PI nanocomposite films. The DS of the (CFE BNNS)/PI nanocomposite films was considerably better without chemical functionalization, DAs, or in situ PAA synthesis. The findings indicate that the most promising PI nanocomposite system that leads to an optimal balance of TC and DS for electric insulation application is the one that uses CFE BNNS as a nanofiller.

References

1. Duffy, Kirsten P.: Electric Motor Considerations for Non-Cryogenic Hybrid Electric and Turboelectric Propulsion. Presented at the AIAA Propulsion and Energy Conference, 2015, pp. 1–10.
2. Chuang, Kathy C., et al.: High Flow Addition Curing Polyimides. J. Polyp. Sci. Part A: Polyp. Chem., vol. 32, no. 7, 1994, pp. 1341–1350.
3. Guo, Hai Quan, et al.: Polyimide Aerogels Cross-Linked Through Amine Functionalized Polyoligomeric Silsesquioxane. ACS Appl. Mater. Interfaces, vol. 3, no. 2, 2011, pp. 546–552.
4. Chuang, Kathy C., et al.: Laser Sintering of Thermoset Polyimide Composites. Presented at the Composites and Advanced Materials Expo, 2019.
5. Weiser, Erik S., et al.: Polyimide Foams for Aerospace Vehicles. High Perform. Polym., vol. 12, no. 1, 2000, pp. 1–12.
6. DeLair, R.: Electrical Insulators. Power Transmission and Conditioning, Edison Tech Center, 2014. http://www.edisontechcenter.org/Insulation.html#wires Accessed Dec. 30, 2024.
7. Wikipedia contributors: Kapton. Wikipedia, The Free Encyclopedia, 2023. https://en.wikipedia.org/w/index.php?title=Kapton&oldid=1187986265 Accessed Dec. 30, 2024.
8. Partridge, Graham: Glass-Ceramics in Biomedical Applications. Adv. Mater., vol. 4, no. 5, 1992, pp. 364–367.
9. Chang, C.W., et al.: Isotope Effect on the Thermal Conductivity of Boron Nitride Nanotubes. Phys. Rev. Lett., vol. 97, no. 8, 2006, p. 085901.
10. Golberg, Dmitri, et al.: Boron Nitride Nanotubes and Nanosheets. ACS Nano, vol. 4, no. 6, 2010, pp. 2979–2993.
11. Lindsay, L.; and Broido, D.A.: Enhanced Thermal Conductivity and Isotope Effect in Single-Layer Hexagonal Boron Nitride. Phys. Rev. B, vol. 84, no. 15, 2011, p. 155421.
12. Ishida, Hatsuo; and Rimdusit, Sarawut: Very High Thermal Conductivity Obtained by Boron Nitride-Filled Polybenzoxazine. Thermochim. Acta, vol. 320, nos. 1–2, 1998, pp. 177–186.
13. Yung, K.C.; and Liem, H.: Enhanced Thermal Conductivity of Boron Nitride Epoxy-Matrix Composite Through Multi-Modal Particle Size Mixing. J. Appl. Polym. Sci., vol. 106, no. 6, 2007, pp. 3587–3591.
14. Shanghai Ping Yiao Trading Co., Ltd.: Boron Nitride PowderGrade PT110. 2010. http://www.pingyiao.com/en/momentive/m2/Boron%20Nitride%20Powder%20Grade%20PT110.html Accessed Dec. 30, 2024.
15. Basal, Narottam P.; Hurst, Janet B.; and Choi, Sung R.: Boron Nitride Nanotubes-Reinforced Glass Composites. J. Am. Ceram. Soc., vol. 89, no. 1, 2006, pp. 388–390.
16. Hung, C-C., et al.: Purifying Nanomaterials. U.S. Patent 8,734,748 B1, May 27, 2014.
17. Hung, Ching-cheh, et al.: Exfoliation of Hexagonal Boron Nitride via Ferric Chloride Intercalation. NASA/TM—218125, 2014. https://ntrs.nasa.gov
18. Rizvi, Reza, et al.: High-Throughput Continuous Production of Shear-Exfoliated 2D Layered Materials Using Compressible Flows. Adv. Mater., vol. 30, no. 30, 2018, p. 1800200.
19. ASTM E1461–01: Standard Test Method for Thermal Diffusivity by the Flash Method. ASTM International, West Conshohocken, PA, 2001.
20. ASTM D149–09: Standard Test Method for Dielectric Breakdown Voltage and Dielectric Strength of Solid Electrical Insulating Materials at Commercial Power Frequencies. ASTM International, West Conshohocken, PA, 2013.
21. Li, Tung-Lin; and Hsu, Steve Lien-Chung: Enhanced Thermal Conductivity of Polyimide Films via a Hybrid of Micro- and Nano-Sized Boron Nitride. J. Phys. Chem. B, vol. 114, no. 20, 2010, pp. 6825–6829.
22. Ciofani, Gianni, et al.: A Simple Approach to Covalent Functionalization of Boron Nitride Nanotubes. J. Colloid Interface Sci., vol. 374, no. 1, 2012, pp. 308–314.
23. Torres Castillo, C.S.; Bruel, C.; and Tavares, J.R.: Chemical Affinity and Dispersibility of Boron Nitride Nanotubes. Nanoscale Adv., vol. 2, 2020, pp. 2497–2506.
24. Fu, Shaoyun, et al.: Some Basic Aspects of Polymer Nanocomposites: A Critical Review. Nano Materials Science, vol. 1, no. 1, 2019, pp. 2–30.
25. Huang, Congliang; Qian, Xin; and Yang, Ronggui: Thermal Conductivity of Polymers and Polymer Nanocomposites. Mat. Sci. Eng. R, vol. 132, 2018, pp. 1–22.
26. Bagchi, Soumendu; Simakov, Evgenya; and Perez, Danny: Formation of Field-Induced Breakdown Precursors on Metallic Electrode Surfaces. Front. Phys., vol. 12, no. 1353658, 2024.